Author/s:
Elahi, Z;Jameson, V;Sakkas, M;Butcher, SK;Mintern, JD;Radford, KJ;Wells, CA

Title:
Efficient generation of human dendritic cells from induced pluripotent stem cell by introducing a feeder-free expansion step for hematopoietic progenitors

Date:
2025-05

Citation:
Elahi, Z., Jameson, V., Sakkas, M., Butcher, S. K., Mintern, J. D., Radford, K. J. & Wells, C. A. (2025). Efficient generation of human dendritic cells from induced pluripotent stem cell by introducing a feeder-free expansion step for hematopoietic progenitors. Journal of Leukocyte Biology, 117 (5), https://doi.org/10.1093/jleuko/qiaf045.

Persistent Link:
https://hdl.handle.net/11343/361871

OXFORD JLB JOURNAL OF LEUKOCYTE BIOLOGY

Journal of Leukocyte Biology, 2025, **117**, qiaf045

https://doi.org/10.1093/jleuko/qiaf045

Methods

Efficient generation of human dendritic cells from induced pluripotent stem cell by introducing a feeder-free expansion step for hematopoietic progenitors

Zahra Elahi,[1] Vanta Jameson,[2] Magdaline Sakkas,[2] Suzanne Kathryn Butcher,[1] Justine D. Mintern,[3] Kristen Jane Radford,[4] and Christine Anne Wells[1,*]

[1]Department of Anatomy and Physiology, Stem Cell Systems, School of Biomedical Sciences, Faculty of Medicine, Dentistry and Health Sciences, The University of Melbourne, Parkville, Melbourne, Victoria 3010, Australia
[2]Department of Microbiology and Immunology, Melbourne Cytometry Platform, School of Biomedical Sciences, Faculty of Medicine, Dentistry and Health Sciences, The University of Melbourne, Parkville, Melbourne, Victoria 3010, Australia
[3]Department of Biochemistry and Pharmacology, School of Biomedical Sciences, Faculty of Medicine, Dentistry and Health Sciences, The University of Melbourne, Parkville, Melbourne Victoria 3010, Australia
[4]Mater Research Institute, The University of Queensland, Translational Research Institute, Woolloongabba, QLD 4102Australia
*Corresponding author: Department of Anatomy and Physiology, Stem Cell Systems, School of Biomedical Sciences, Faculty of Medicine, Dentistry and Health Sciences, The University of Melbourne, 30 Royal Parade, Parkville, Melbourne, Victoria 3010, Australia. Email: wells.c@unimelb.edu.au.

Abstract

Dendritic cells (DCs) are rare innate immune cells that are essential regulators of antitumor, antiviral, and vaccine responses by the adaptive immune system. Conventional DCs, particularly the cDC1 subset, are most desired for DC-based immunotherapies, however, it can be difficult to isolate sufficient numbers of primary cells from patients. The most common alternate sources of DC are *ex vivo* monocyte-derived DC, although patient-derived monocytes are often dysfunctional. Induced pluripotent stem cells (iPSC) offer a promising solution, providing an opportunity for in vitro generating DCs that are suitable for allogenic off-the-shelf batch-manufactured cells. Here, we developed an in vitro protocol designed to maximize the yield of iPSC-derived DC progenitors, with the specific goal of generating cDC1-like cells. The iPSC-DCs subsets generated by our method could be partitioned by cell surface phenotypes of cDC1, cDC2, and DC3, but they were most transcriptionally similar to monocyte-derived DC (MoDC). Stimulated iPSC-DCs generated proinflammatory cytokines, expressed migratory chemokine receptors including CCR7, upregulated co-stimulatory molecules, and induced the proliferation of CD4/CD8 T-cells. Altogether these data indicate that iPSC-derived DCs have the potential to traffic through lymphatic endothelium and engage productively with T-cells. This method offers a promising step toward an expandable source of allogeneic human DCs for future applications.

Keywords: cDC, dendritic cell, hematopoietic progenitor, induced pluripotent stem cell, MoDC

1. Introduction

Dendritic cells (DC) are specialized antigen-presenting cells that traffic to lymph nodes, where they efficiently activate naïve CD4+ and CD8+ T lymphocytes. They can perform both conventional presentation and cross-presentation (presenting exogenous antigens through MHC-I molecules) of antigens to T cells and therefore are the target cell types for most vaccines.[1] DC-based vaccines have shown sporadic but highly effective potential in anticancer immunotherapies for late-stage melanoma,[2] glioma[3] and other aggressive tumors (reviewed by Wculek et al.[4]).

Among the heterogenous population of DCs, the cDC1 subset has an exceptional ability to cross-present tumor antigens to CD8+ T cells and induce an efficient antigen-specific response.[5,6] Murine cDC1 displayed a higher capacity to activate and induce the proliferation of CD8+ T cells than cDC2 and MoDC subsets[7] and were shown to be the only antigen-presenting cells able to transport intact tumor antigens to the tumor-draining lymph nodes and prime CD8+ T cells.[8] However, the clinical application of human cDC1, such as cDC1-based cancer vaccines, is fundamentally limited by their scarcity in circulation, short half-life, and poor proliferative abilities. The development of DC-based vaccines is further hindered by dysregulation of patient-derived DCs,[9] the poor ability of primary DC and monocytes to proliferate in culture, and time sensitivities implicit when expanding DC from progenitors.

Currently, the most common approach for producing clinical-grade DCs is the *ex vivo* differentiation of monocytes to DCs. To obtain Monocyte-derived DC (MoDC), the CD14+ fraction of peripheral blood mononuclear cells (PBMC) is isolated and treated with IL4 and GM-CSF for several days.[10] MoDCs show a typical dendritic morphology and express MHC class I and class II molecules, CD172a, CD1a, CD1c, and CD11c (reviewed by[11]) with variable CD14 expression.[12,13] MoDCs matured with LPS and TNFα have enhanced expression of MHC II and co-stimulatory molecules and generate high levels of proinflammatory cytokines with the capacity to induce naïve CD4+ T cell differentiation.[14] MoDCs have

Received: May 22, 2024. **Revised:** February 18, 2025. **Accepted:** April 11, 2025. **Corrected and Typeset:** May 20, 2025

been the cell of choice for many clinical studies using autologous DC-based vaccines.[15] However, monocytes and MoDC are short-lived cells,[16,17] and the number of MoDC available is fundamentally constrained by the number of monocytes that can be isolated from a donor, impacting their manufacturing or delivery for clinical use.

An alternate source is the differentiation of CD34+ hematopoietic stem cells isolated from cord blood (CB-HSC). These cultures are able to support the differentiation of multiple DC subsets, such as CLEC9A+ cDC1,[18,19] CD123+ pDC, CD1c+ cDC2, and MoDC.[20,21] Nevertheless, one of the challenges associated with the generation of DC, particularly cDC1 subset, from CB-HSC is the low yield of differentiation.[18,22,23] Transcriptionally, we have shown that CB-DC captures an immunoregulatory profile (mregDC),[22] which leads to less efficiency in anticancer responses due to the induction of many regulatory genes.[24] While the phenotype of these cells partially matches the primary cDC1 or cDC2, manufacturing of CB-cDC remains a major limitation when seeking to generate sufficient DCs for clinical application.

Pluripotent stem cells offer another source for DC derivation, and 2 broad approaches have been reported. The first and most common approach uses embryoid bodies (EB) to produce hematopoietic stem cell (HSC) followed by differentiation toward terminal DCs in a feeder-free culture setup. The absence of feeder cells in this method makes it a well-defined process; however, it typically generates low numbers of monocyte- and cDC2-like cells from iPSC[25–27]. Alternatively, co-culture of iPSC with mouse stromal cells engineered to express Notch ligand DLL1[28] has been reported to produce cDC1-like cells. Although this approach derived a high percentage of cDC1, the use of mouse feeder cells introduces xenogeneic components to the system, which compromises clinical applicability. Here, we sought to increase the yield of the feeder-free EB-based method for scalable generation of iPSC-derived HSC that efficiently differentiate into multiple iPSC-DC subsets capable of activating T-cells.

2. Materials and methods

2.1 Cell lines and ethics

All works conducted on primary human cells, and iPSC lines were overseen by the University of Melbourne HREC under approvals 1646608 and 2023-28021-46872-3.

Primary CB cells were obtained through the BDMI CB bank at the Royal Children Hospital, Melbourne.

This study also used 2 human iPSC cell lines previously described[29] including PB001.1 (hPSC reg: MCRIi001-A; RRID: CVCL_UK82),[30] obtained from the Stem Cell Core Facility at the Murdoch Children's Research Institute and HDF51[31] (RRID: CVCL_UF42), which was a gift from Professor Andrew Laslett, CSIRO.

2.2 iPSC maintenance and expansion

iPSCs were cultured in supplemented E8 media (Thermo Scientific, #A1517001) on Matrigel Matrix (Thermo Scientific, #354277) coated dishes. To coat the dishes, 1 mL of frozen Matrigel aliquot was thawed at 4 °C overnight. Thawed Matrigel was diluted 1/50 in cold E8 media and was then added to the cell culture dishes (Merck, #Z755923). Coated dishes were incubated at room temperature for 1 h and used immediately or kept in the fridge for later application.

Seeded iPSC cells were maintained in a humidified incubator at 37 °C with 5% CO2 and spent media was replaced with fresh supplemented E8 daily. To passage cells when confluent at 70% to 80%, cells were first washed with PBS (Thermo Scientific, #10010023), then incubated with 1/1000 EDTA (Thermo Scientific, #15575020) in PBS buffer for 3 to 4 min at 37 °C with 5% CO2 to allow detachment. After incubation, the buffer was gently removed, and cells were detached by pipetting using fresh E8 media. Detached cells were collected in a 15 mL centrifuge tube (Corning, #430791), spun at 300 g for 5 min, and reseeded at one-fourth dilution.

2.3 EB formation and differentiation

EB culture medium was based on STAPEL media[32,33] (Table S1). To generate EBs, iPSC cells were detached enzymatically using cell release buffer (1/1000 EDTA/PBS), and clumps of cells were collected by pipetting using EB media (Table S1) supplemented with differentiation factors for day 0 to 1 (Table S2). Collected cell clumps were filtered through 70 µm-sized strainers into a 50 mL sterile tube. Cell clumps were removed by 10 mL serological pipettes and added gently to an ultra-low attachment culture dish (Sigma Aldrich, cat#CLS3261) to be maintained at 37 °C with 5% CO2 placed on an orbital shaker (SCIENTIFIX, cat#NBT-101SRC) rotating at 32 rpm. For each 100 mm dish, 2 to 3×10^6 cells were used for EB formation. Media change strategy, including the details of each differentiation factor, is described in Table S2. To improve cell viability at the EB formation step, 0.2 nM ROCK Inhibitor Y-27632 (Stemcell Technologies, #72307) was added to the media from day 0 to 1 and discontinued since then. From Day 7, iPSC-derived hematopoietic cells started to emerge from EB as suspension cells.

2.4 iPSC-derived progenitor expansion

Progenitor cells that emerged from EBs were collected and spun at 300 g for 5 min. Collected cells were resuspended in 1 mL of prewarmed amplification media described in Table S3. Cells were cultured in 100,000 cell/mL density on T25 cell culture flasks and incubated at 37 °C with 5% CO2. Cells were expanded 4 to 7 d based on the experimental design. During expansion, media was not changed.

2.5 iPSC-derived DC differentiation

Expanded progenitors were collected and spun at 300 g for 5 min. 200,000 cell/mL were seeded on T25 tissue culture flasks in DC differentiation media described in Table S4. At day 6, half of media was replaced with fresh differentiation media with 2× concentration of cytokines.

2.6 CB CD34+ HSC-derived DC differentiation

The CD34+ HSC cells were isolated using Human Cord Blood CD34 Positive Selection Kit II (Stemcell Technologies, #17896) as per the supplier instruction. Briefly, first step of enrichment used RosetteSep cocktail to deplete platelets. Then CB were diluted 1:1 (v/v) into a dilution buffer (1 mM EDTA in PBS supplemented by 2% FBS (Thermo Fisher, #10099141)) and undelayed with density gradient medium LymphoPrep (Stemcell Technologies, #07801). The mix was centrifuged at 1200 × g for 20 min with no brake. Blood mononuclear cells (BMC) were harvested from the interface layer between plasma and red cells and spun at 300 × g for 10 min with no brake. The cell pellet was diluted 1:1 (v/v) in DB and transferred to a 5 mL round bottom polystyrene tube (Stemcell Technologies, #38030). CD34+ cells were enriched by magnetic selection using Selection antibody cocktail in the kit. Isolated cells were plated in amplification media (Table S3) for 4

to 7 d. Expanded cells were harvested and used for characterization, freezing or proceeding to the differentiation phase. For the latter purpose, cells were cultured in DC differentiation media (Table S4) for 11 d; at day 6, half of the media was replaced with fresh media containing 2× concentration of cytokines.

2.7 Flow cytometry analysis

Immunophenotyping and FACS were performed on primary cells and differentiated cultures. First cells were incubated inhuman FcR Blocking Reagent (Miltenyi Biotec, #130-059-901), 5 min at RT, then resuspended in 200 µL staining buffer and incubated with antibodies (see Table S5) for 20 min in the dark at 4 °C. Cells were washed with cold staining buffer 3 times and filtered through 70 µm filters. Cells were sorted into collection buffer consisting of 50% FBS (Thermofisher, #10099141) in HBSS (Thermofisher #14175103) using a BD FACS ARIA III/FACS DiVa version 9 software (Becton Dickinson, Franklin Lakes, NJ) fitted with a 100 um nozzle at 20 psi. For immunophenotyping, CytoFLEX LX/CytExpert software (Beckman Coulter, Brea, CA) was used to acquire samples. Post-acquisition analysis was performed using FCS Express v7 software (De Novo/Dotmatics, Boston, MA).

2.8 Stimulation assay

Differentiated CD11c+ CD1c+ cells from iPSC cell lines and CB donors were FACS sorted (Table S5) and stimulated with a combination of 1 µg/ml LPS (InvivoGen, #tlrl-smlps), 5 µg/mL HMW poly(I:C) (InvivoGen, #581942011) and 5 µg/ml R848 (InvivoGen, #tlrl-r848) in the 24-well tissue culture plate. After 16 h, cells were collected and analysed by flow cytometry for the expression of HLA-DR and co-stimulatory molecules (CD40, CD80, and CD86) (Table S5). The supernatant was collected for the cytokine bead assay (CBA) and was processed at the Hudson Institute, Monash University. The fluorescent intensity data for each cytokine was received, and an associated standard curve was generated. A multiparameter regression model was fit to the standard curve and was used to calculate the concentration (pg/mL) of each cytokine.

2.9 Real time qPCR assay

mRNA extraction of samples was carried out using Qiagen RNeasy Plus micro Kit (Qiagen, cat#74034) and was transcribed into cDNA using Fast SYBR Green Master Mix (Thermo Fisher Scientific, #4385612), according to the manufacturer instructions. RT-qPCR was performed using the ViiA7 QRT-PCR machine (Applied Biosystems). Relative gene expression was calculated using ΔCT method normalized to human B2M housekeeping gene (See Table S6).

2.10 Mixed leukocyte reaction test

Pan CD4/CD8 T cells were isolated from healthy PBMC donors using PAN T CELL ISOLATION KIT HUMAN, Miltenyi Biotec (130-096-535) according to the manufacturer's instructions. After 24 h, T cells were stained with 5 µm CellTrace CFSE Cell Proliferation dye (Thermo Fisher, #C34554), according to the manufacturer's instruction. Terminally differentiated iPSC-DCs were harvested and collected in a 15 cm tube. 10,000 iPSC-DC were added to each well of 96-well round bottom plate and incubated 15 min at 37 °C with 5% CO2. 10×10^5 of CFSE-labeled T cells were added on top of DCs in RPMI supplemented with 10% FBS, 100 ng/mL LPS (InvivoGen, #tlrl-smlps), 5 µg/mL HMW poly(I:C) and 100 ng/mL rh GM-CSF. Control wells had only 10×10^5 T cells in RPMI supplemented with 10% FBS. Samples were assessed for the intensity of CFSE by flow cytometry.

2.11 RNA-seq experiment

Human iPSC-derived cDC1 and cDC2 subsets from 2 iPSC cell lines, and CB-derived subsets from 3 healthy donors were FACS sorted as Live HLA-DR+ CD14− CD141+ CLEC9A+ cDC1, Live HLA-DR+ CD14− CD11c+ CD1c+ DC2A and Live HLA-DR+ CD14+ CD11c+ CD1c+ DC2B subsets. Minimum 200×10^3 cells were collected for each sample and lysed in lysis buffer provided by Qiagen RNeasy Plus micro Kit (Qiagen, cat#74034) proceeded by extracting RNA using the manufacturer instructions. RNA quality determined by RNA Integrity Number (RIN^e) and quantity was determined by High Sensitivity RNA ScreenTape (Agilent) using Agilent 2,200 Technologies Tapestation System. RNA samples were processed as described previously[34] by MHTP Medical Genomics Facility at the Monash Health Translation Precinct. Pooled libraries from 3 batches were sequenced with Illumina NSQ2000 with a mean size of ~493 bp paired-end reads and ~550 M reads/run.

2.12 RNAseq data analysis

FASTQ files were obtained from the sequencing facility and were processed using the standard Stemformatics data processing pipeline.[35] Raw counts were analysed using the Limma package.[36] Low-count genes were filtered using the default settings of the filterByExpr function from EdgeR[37] while counting for the variance between biological groups. Filtered counts were normalized to logCPM and used for further analysis. A voom plot was used to assess the quality of filtering. Clustering of samples was done using plotMDS. Ggplot2[38] was used to generate violin and box plots. Bulk mRNA-sequencing data is available through accession GSE261731.

2.13 Differentially expressed gene analysis

Statistical differentially expressed (DE) analysis was performed using R. The differential gene expression analysis between 2 groups of samples coming from different batches was performed using linear mixed-effect models by the lmer function from the lme4 package.[39] In this modeling, the variable of interest and the batch parameter were considered as random effects. Benjamini-Hochberg (BH) adjustment was used for the *P*-value correction method. The genes with *P*-adjust < 0.05 and logFC > 1 were selected as DE genes. Code is available from the Wells laboratory GitHub: https://github.com/wellslab/DC_bulkRNA-seq_ZahraElahi.

2.14 Projection method

The projection of RNA-seq data to the reference Stemformatics DC atlas has been described previously.[35] The projection vignette is provided on the Stemformatics.org atlas website.

3. Results

3.1 Establishing an EB-based iPSC differentiation method to generate human DC subsets

We first set out to assess 2 approaches for in vitro DC generation, including 1 previously reported from human iPSC by Sachamitr et al.[40] and 1 from human cord blood (CB) CD34+ progenitors by Balan et al.[18] here referred to as Sachamitr iPSC and Balan CB methods, respectively. The Sachamitr iPSC differentiation

method required a 2-wk-long culture to generate hematopoietic progenitors (iPSC-HSC) from EB in a growth factor cocktail that included GM-CSF from the beginning and then a further 10 d to differentiate these progenitors to iPSC-DC using GM-CSF and IL4 (Fig. 1a). The Balan CB method included a 7-day amplification step of HSCs, then differentiation in a panel of FLT3-L, GM-CSF, and IL-4 to derive DCs (Fig. 1b).

We designed a new protocol, referred to as the iPSC Elahi method, which combines a modified version of a contemporary EB method[29] with an amplification step of the HSC progenitors inspired by Balan et al.[18] (Fig. 1c). Our modified 4-step protocol used a brief pulse of CHIR to induce mesodermal differentiation in iPSC, then patterned EB with BMP4, SCF, and VEGF before introducing FLT3L and IL3 to promote the production of CD34+ CD45+ HSC progenitors. We collected iPSC-derived HSC cells on day 7 of EB formation, and expanded these in FLT3L, TPO, IL3, and SR1 for 4 d (Fig. 1d) to increase the number of iPSC-HSC and DC progenitors. DCs were then differentiated in media containing FLT3L, SR1, GM-CSF, and IL4 for up to 2 wk.

The Sachamitr iPSC protocol did generate ~18% CD34+ CD45+ cells at day 13, indicating specification to a hematopoietic cell type, but with low numbers of HSCs harvested ($<300 \times 10^3$ cells per 10 mL batch) with 30% viability (Fig. 1d–f). In contrast, the Balan CB method showed a 40% CD34+ CD45+ HSC yield, generating $>5 \times 10^6$ progenitors with 95% viability (Fig. 1d–f). Despite implementing multiple levels of improvement to the iPSC Sachamitr protocol, the quantity of generated HSCs by this method still fell significantly short of those produced by the CB method (described in Table S7 and Fig. S1). We were motivated to develop a new iPSC protocol that generates a similar or even higher proportion of HSC progenitors than the CB method. Our method (Elahi iPSC) significantly enhanced the yield of the CD34+ CD45+ HSC generation by up to 54% and increased their number to more than 10-fold compared with the previous Sachamitr iPSC method (Fig. 1d–f). However, the number and the viability of generated HSC were similar between our method and the CB differentiation approach (Fig. 1d–f).

Assessing the terminally differentiated DC from our expanded iPSC-HSC, we observed that 2×10^6 of iPSC-HSC yielded 10% to 12% cDC1-like cells expressing CLEC9A+ CD141+, of which we routinely generated 1.8×10^3 cDC1 per batch of 10 mL media, and an equivalent number of cDC2-like cells expressing CD11c+ CD1c+ (Figs. 2 and S2). This was more than the number of cDC2 and equivalent to cDC1 obtained from the Balan CB method in our hands. The proportion of cDC-like subsets obtained from the Sachamitr protocol was significantly lower than that of our protocol. The high number of DCs obtained by the Elahi iPSC method was greatly enhanced by increasing the number of progenitors available for differentiation. From this point forward, we stopped characterizing the Sachamitr method, and any DCs derived from Elahi iPSC method will now be referred to as iPSC-DC.

3.2 CD11c$^+$ cells differentiated from iPSC in vitro cannot be efficiently generated by FLT3L alone

We next sought to optimize the number of FLT3(CD135)+ CD11c+ DC. Four conditions were tested using 2 different iPSC lines (HDF51 and PB001.1). FL: 100 ng/mL FLT3L alone; FLG: FL+ 20 ng/mL GM-CSF; FLI: FL+ 20 ng/mL IL4 or FLGI which combined all 3 cytokines. FLT3L alone did not efficiently generate CD11c+ cells (Fig. 3), however, in combination with GM-CSF, gave rise to 5% CD11c +cells. The most efficient combination was FLGI culture, which gave rise to 14.8% CD135+ CD11c+ cells, showing that the combination of GM-CSF and IL-4 is more efficient for the development of the iPSC-DC. We then sought to find the optimum concentration of these cytokines. Increasing the amount of GM-CSF/IL4 relative to FLT3L from 5 ng/mL to 50 ng/mL promoted the generation of CD14+ cells, whilst the proportion of CD141+ cells remained the same (Fig. 3c). We, therefore, set the optimum concentration of GM-CSF and IL4 for iPSC-DC differentiation at 5 ng/mL.

3.3 iPSC-cDC subsets derived in vitro are phenotypically heterogeneous

To investigate the identity of the DCs derived from iPSC in vitro, we ran a flow cytometric analysis on cells at day 23 of differentiation. We used a panel of antibodies, including HLA-DR, CD11c, CD141, CLEC9A, CD1c, and CD14, in addition to the viability stain. To combat highly auto-fluorescent (AF) cells, we introduced gating steps in short and long wavelengths to remove them (Fig. 4a). The iPSC-derived cDC1-like subset was characterized as live HLA-DR$^+$ CD14– CD11c$^{mid/+}$ CD141+ CLEC9A+.

The iPSC-derived cDC2-like subset was characterized as live HLA-DR$^+$ CD11c+ CD172a+ CD1C+ cells. This population was heterogeneous in terms of the expression of CD14, including CD1c+ CD14– and CD1c+ CD14+ groups (Fig. 4a). CD1c+ CD14+ cDC2 showed a greater level of CD11c expression than CD1c+ CD14– cDC2, while the level of HLA-DR expression was similar (Fig. 4b). The CD14+ population was slightly larger by having a higher area of the forward scatter signal (FSC-A). They also had marginally more granularity than CD14– cDC2, measured by the side scatter signal (SSC).

3.4 iPSC-derived dendritic cells (iPSC-DCs) are not transcriptionally equivalent to primary cDCs

To understand the biology of iPSC-derived DC (iPSC-DC) subsets and to investigate their similarity with cord blood-derived DC (CB-DC) equivalents, we sorted each subset and analysed them through RNA-sequencing (Fig. 5a). Both CB-derived DC and iPSC-DC were expanded at the progenitor stage for 4 d before differentiation. The cDC1 subset was sorted as live HLA-DR$^+$ CD14– CD11c$^{mid/+}$ CD141+ CLEC9A+. Two populations of DC2 were sorted as live HLA-DR$^+$ CD11c+ CD172a+ CD1C+ with negative or positive expression of CD14 referred to as DC2A and DC2B, respectively. At least 200×10^3 cells were sorted for each sample with replicates from 2 different iPSC cell lines and from 3 CB donors, noting that the cDC1 population from 1 CB donor failed RNA QC because of low cell numbers.

We first examined the sample clustering using a multidimensional scaling (MDS) plot. The first dimension (dim 1) accounted for 27% of expression variability and defined subsets of iPSC-DC2A and iPSC-DC2B, respectively. The second dimension accounted for 19% of expression variability and described the difference between iPSC-DC1 and iPSC-DC2 s (Fig. 5b). In contrast, the CB-DC1 and DC2 subsets were captured on dim 1, 29% of expression variability, while dim 2 (20% variability) separated CD14+ and CD14– cells (Fig. 5c).

Next, we identified the DE genes that separated subsets within the iPSC-DC groups (Table S9). The 10 most discriminating genes ranked by LogFC were chosen for illustrative purposes (Fig. 5d). The genes highly expressed by iPSC-DC1 were closely related to the maturation and migration of DCs (eg *MYCL, CXCL1, ZDHHC1, SEMA3C, NR4A3*) and the antigen presentation process (eg *TEAD4, ERAP2, AP1S1*). iPSC-DC2A upregulated genes involved in communication with T cells (eg *THBS1, FCER1A, CD1D*) and

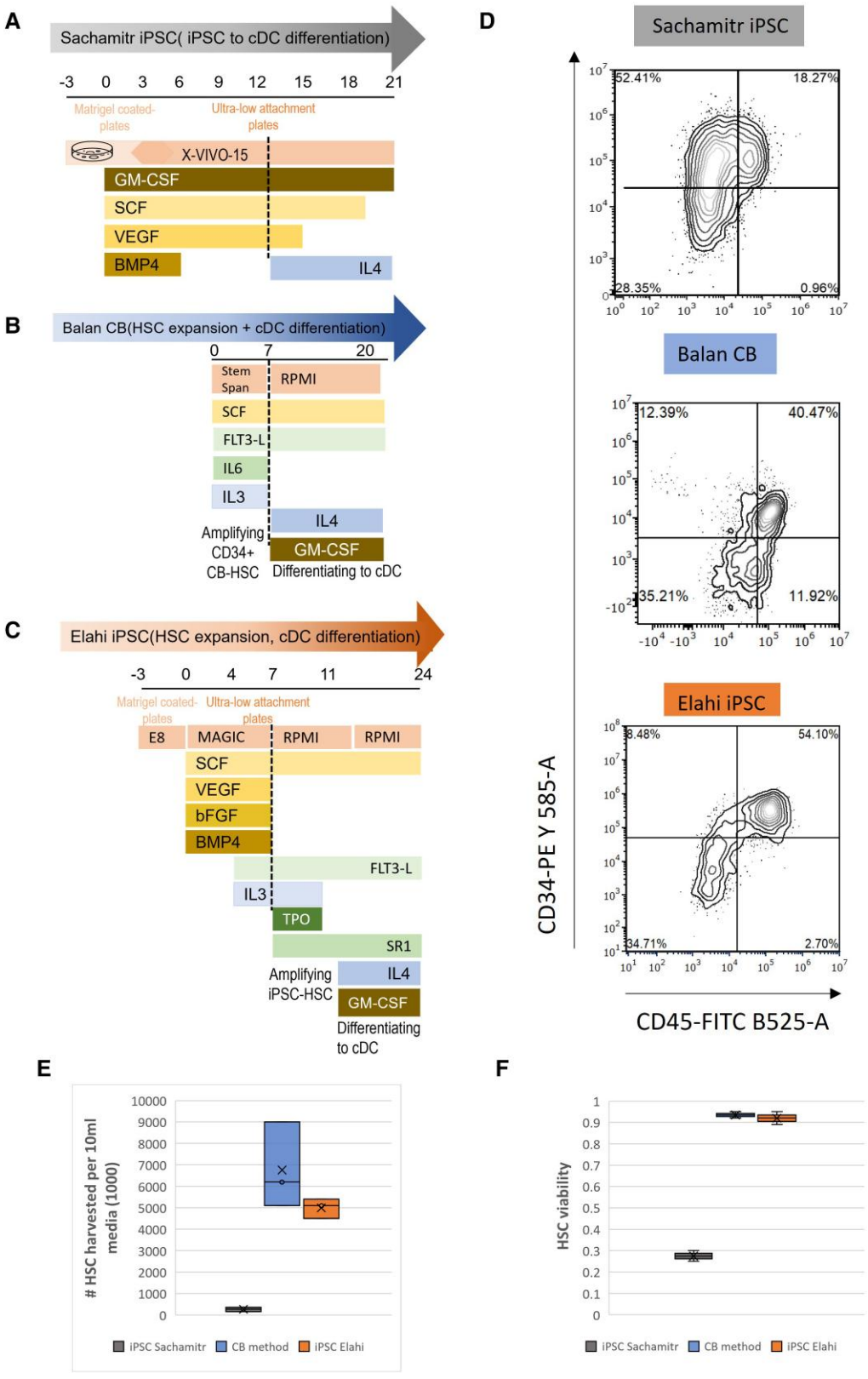

Fig. 1. Generating hematopoietic progenitors of DCs in vitro. a) Schematic overview of a replicated iPSC-DC differentiation method developed by Sachamitr et al.[40] b) differentiation protocol of CB-progenitors toward DC developed by Balan[18] with minor modifications. c) Our new developed differentiation protocol of iPSC toward DC (iPSC Elahi method). d) Flow cytometric assessment of harvested hematopoietic stem cells HSCs from each method for the expression of CD34 and CD45 markers. The e) number and f) viability of harvested HSCs from each method per batch of 10 mL media. Data are representative of 3 replicates of 2 iPSC cell lines (PB001.1 and HDF51) and 3 individual cord blood donors (summarized at Table S8).

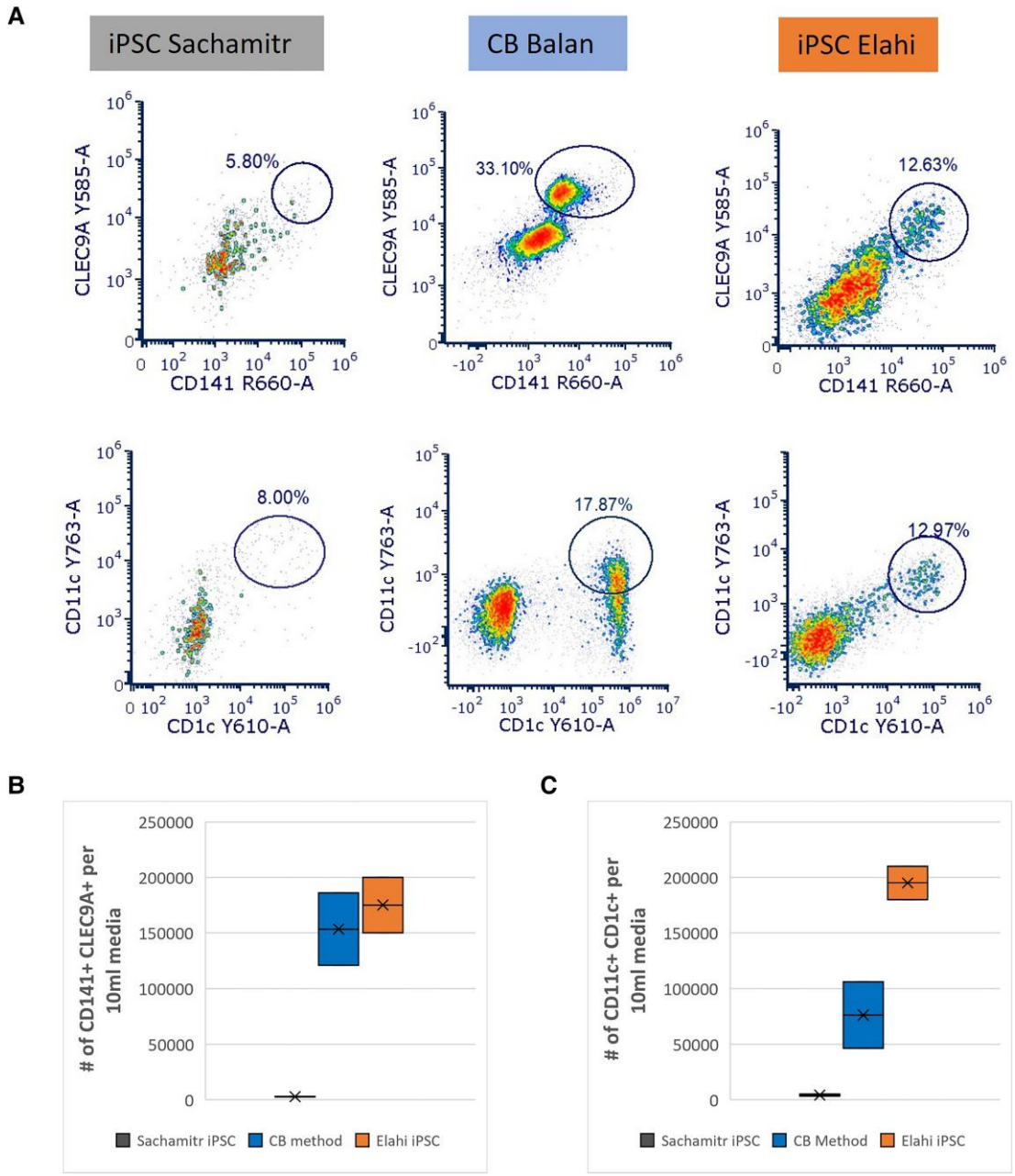

Fig. 2. New developed protocol is more efficient in producing iPSC-derived conventional DCs. a) The flow cytometry analysis of terminal differentiated cDCs comparing the percentage of the differentiated Live CD141+ CLEC9A+ cDC1 (top) and Live CD11c+ CD1c+ cDC2 (bottom) between the replicated Sachamitr protocol, CB method and our new developed protocol (Elahi iPSC). Isotype control samples are shown in Figure S2. b) Box plot showing the number of differentiated CD141+ CLEC9A+ cDC1 and c) CD11c+ CD1c+ cDC2 per 10 mL media compared across multiple protocols including Sachamitr protocol, CB method and our new developed protocol (Elahi iPSC). Data is from 2 replicates of PB001.1 iPSC cell line and 2 replicates of 1 CB donor.

iPSC-DC2B showed upregulation of cytokine signaling genes (eg *CD28, IL10, TNFSF12, IL15RA*). We asked whether genes that exhibit distinct expression patterns in iPSC-DC subsets also demonstrate subset-specificity across DC subsets derived in vivo. Our analysis, leveraging the Human DC Atlas database,[41] revealed that most of these genes do not display subset-discriminating patterns among in vivo DCs (Fig. S3a).

Investigating the differential expression profile of the CB-derived DCs showed high expression of cDC1 markers *CLEC9A, IRF8, CADM1*, and *XCR1* by CB-DC1 subset (Fig. 5e, Table S10). In contrast, a partial cDC1 identity was obtained from iPSC-DC1. Expression of *CLEC9A* and *CADM1* was slightly higher, but not significantly, in iPSC-DC1 compared with iPSC-DC2A/B, while all subsets lacked expression of *IRF8* and *TLR3* (Fig. S3b). The level of *CLEC9A* transcript expression by iPSC-DC1 was significantly lower than CB-DC1 (Fig. 5f). CB- and iPSC-derived DC1 cells expressed high levels of the *CD1C* gene, which is a common marker of the cDC2 subset (Fig. 5g). Altogether, iPSC-derived DCs captured a transcriptional identity that was different from CB-derived or primary DC equivalents.

We then examined the projection of the sequenced samples to the reference Human DC Atlas. The iPSC-DC subsets strongly clustered and showed transcriptional similarity with the in vitro (Mo-DC) samples (Fig. 6a and b). To determine whether iPSC-DC,

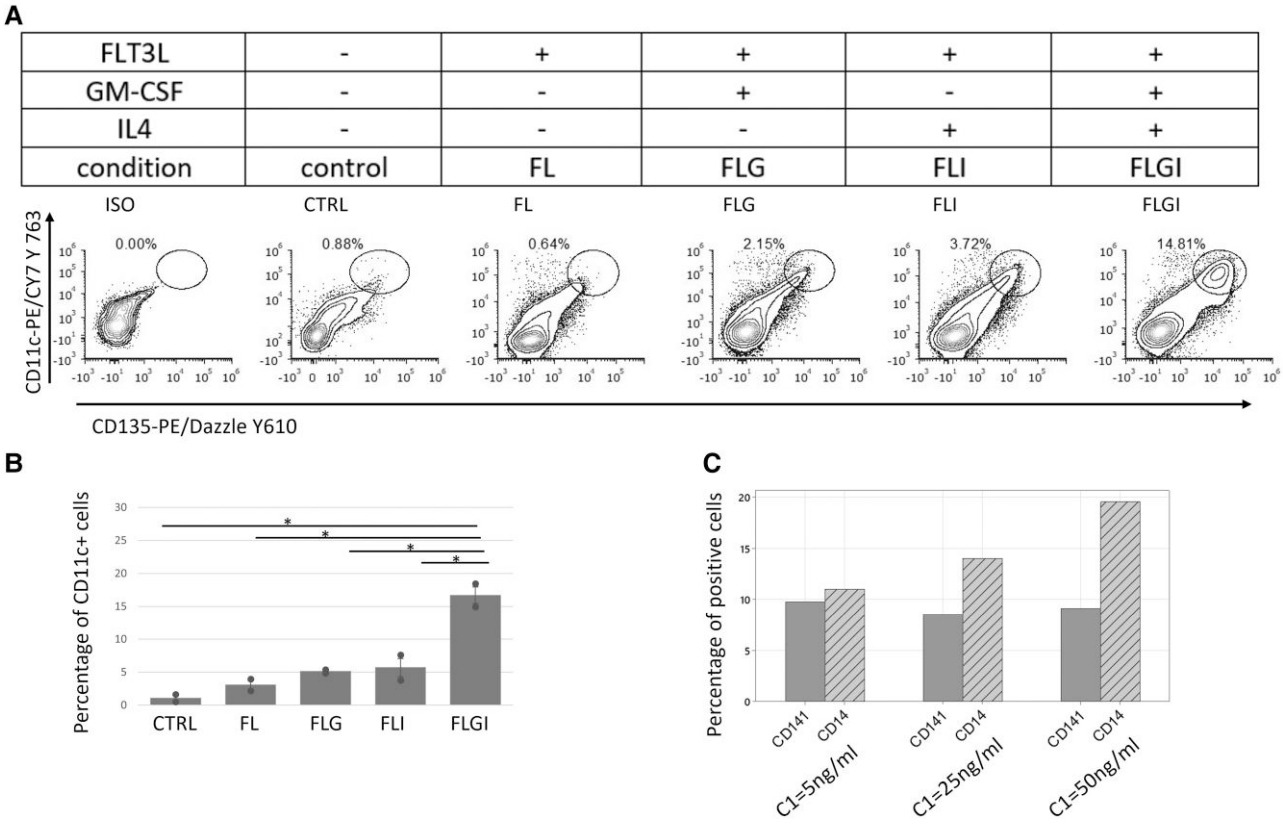

Fig. 3. The in vitro differentiation of CD135+ CD11c+ cells require a combination of GM-CSF and IL4 cytokines on top of the FLT3 ligand. a) Representative flowcytometric plots assessing the yield of CD11c +generation under 4 conditions including FL (100 ng/mL FLT3L), FLG (100 ng/mL FLT3L+ 20 ng/mL GMS-CF), FLI (100 ng/mL FLT3L+ 20 ng/mL IL-4), FLGI (100 ng/mL FLTL3+ 20 ng/mL GM-CSF+ 20 ng/mL IL-4) and control (no FLT3/GM-CSG/IL4). ISO refers to the isotype control sample. b) The bar graph compares the percentage of CD11+ cells under the 4 conditions mentioned earlier. Data were obtained from 2 iPSC cell lines, PB001.1 and HDF51. (*$P < 0.05$, paired 2-tailed student *T*-test). c) The grouped bar graph showing the percentage of CD141+ and CD14+ cells differentiated under 3 different concentrations of GM-CSF/IL4, including C1:5, C2:25, and C3:50 ng/mL. In all conditions, FLT3L is present at 100 ng/mL.

with a monocytic profile, are distinct from the iPSC-derived macrophages (ipMAC), we combined our dataset with another RNAseq dataset from our laboratory[29] that has profiled ipMAC and macrophages differentiated from blood monocytes (MDM). To be consistent with our cells, the samples selected from this dataset were nonactivated control MDM and ipMAC samples. Previously, IRF4 and MAFB transcription factors were discovered to distinguish human MoDC from MoMAC and vice versa.[42] Consistent with this finding, our iPSC-DCs showed higher expression of *IRF4* but lower *MAFB* compared with ipMAC and MDM (Fig. 6c and d).

3.5 iPSC-derived DCs respond to TLR stimulation as efficiently as CB-DC2s

To examine the capacity of iPSC-DC and CB-DC to activate T-cells, we first assessed their response to microbial stimuli. Using a combination of LPS, Poly I:C and R848 (referred to as LPR stimuli), which are commonly used to test DC maturation, FACS-sorted CD11c+ CD1c+ iPSC-DC and Cd11c +CD1c+ CD14– CB-DC2A were stimulated overnight (16 h), and secreted immune modulators measured by CBA. Upon stimulation, both iPSC-DC and CB-DC2 secreted proinflammatory cytokines. TNFα, IL-6, and IL-8 proteins were detected at high levels and IL-1 (IL-1a and IL-1b) at lower levels (Fig. 7), patterns that are consistent with known functional[43,44] characteristics of cDC2 s. The nonstimulated (control) CB-DC2 samples were secreting a moderate level of TNFα, IL-8, and IL-1a protein, suggesting a level of preactivation. In contrast, control iPSC-DC showed no inflammatory profile.

The ability of iPSC-DC to increase expression of HLA-DR, co-stimulatory molecules and chemokine receptors in response to TLR stimuli was next assessed (Fig. 8). CD86 and HLA-DR expression were present at high levels in the unstimulated iPSC-DC, and although we saw a modest shift in some cells on stimulation, this was not statistically significant (Fig. 8a). In contrast, robust upregulation of CD40 and CD80 following activation, with a median fluorescent intensity (MFI) approximately double that of unstimulated samples was observed (Fig. 8a). Given that we also observed a significant upregulation of mRNA expressed from the migration-associated gene, *CCR7*, and the corresponding CCR7 surface marker by iPSC-DC after stimulation compared with the control unstimulated samples (Fig. S4), we concluded that in vitro-derived DCs generated from iPSC by our method are mature and functionally responsive to microbial ligands recognized by the TLR family.

To evaluate the capacity of iPSC-DCs to interact with T cells, we used a mixed leukocyte reaction (MLR) test. Stimulated iPSC-DCs were co-cultured with pan-CD4/CD8 T cells, and the proliferation of T cells was assessed after 7 d using a cell division tracking dye, CFSE. We found that iPSC-DCs were able to reliably induce proliferation in 20% to 25% of the T-cells ($P > 0.0001$, Fig. 8b), whereas the control T-cell condition lacking iPSC-DC was not proliferative.

4. Discussion

We designed and developed an optimized protocol for generating human DCs from iPSC in a feeder-free differentiation approach.

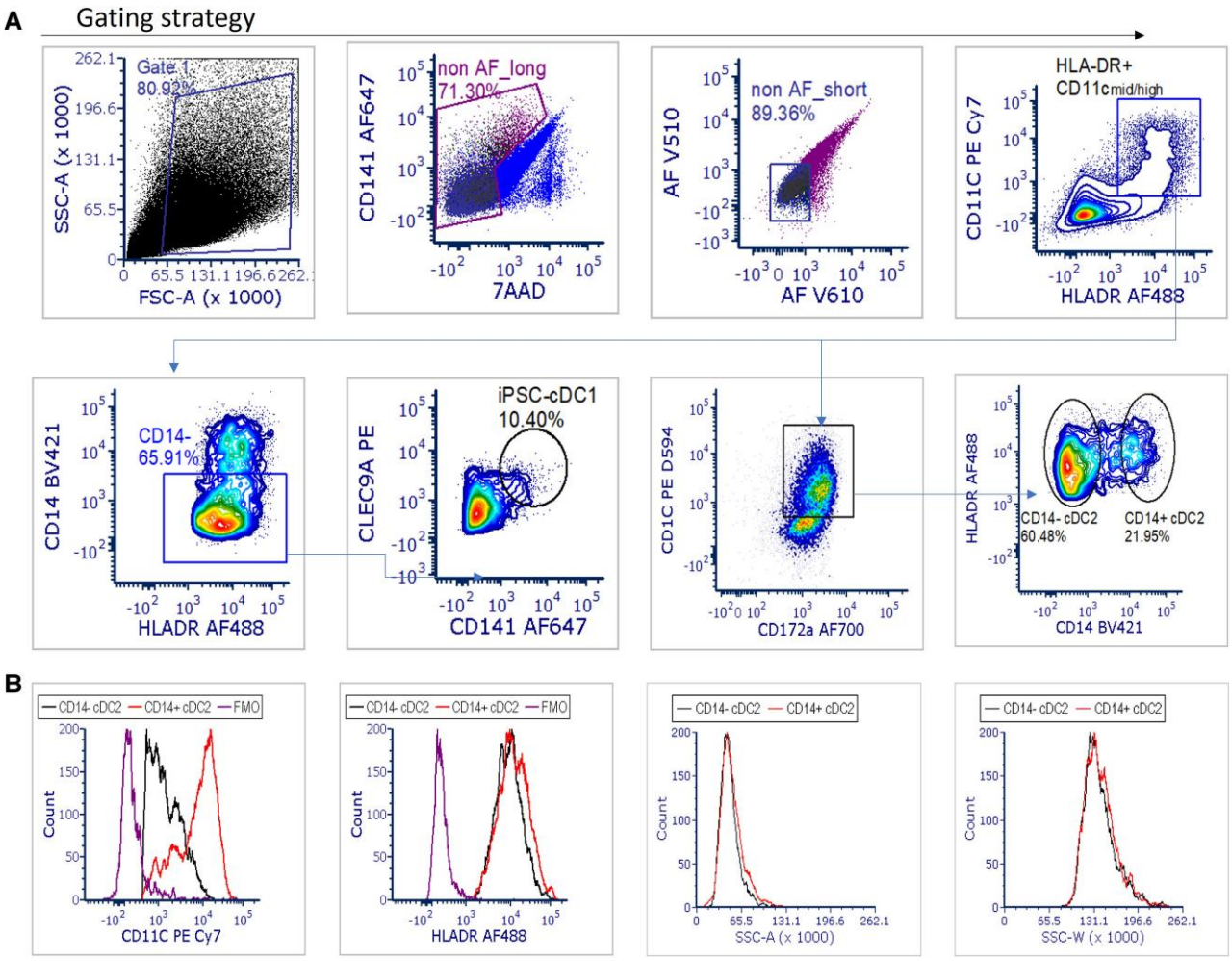

Fig. 4. Flow cytometric characterization of differentiated iPSC-cDC subsets. a) AF cells were removed from further analysis during 2 steps. iPSC-cDC1 and iPSC-cDC2 were characterized as Live HLA-DR$^+$ CD14− CD11c$^{mid/+}$ CD141+ CLEC9A+ and Live HLA-DR$^+$ CD11c+ CD172a+ CD1C+ cells, respectively. b) Assessment of iPSC-derived CD14+ cDC2 and CD14− cDC2 subpopulation regarding their differences in CD11c and HLA-DR expression levels. The area and width of the side scatter signal (SSC-A and SSC-W) represent their size and granularity, respectively. CD14+ population is in red, CD14− in black and the FMO (full −1) control in purple.

Our method incorporates an amplification phase of iPSC-derived myeloid progenitors, resulting in an improved differentiation yield and a greater number of iPSC-derived DCs compared with a previous iPSC method and similar to the yields obtained from CB *ex vivo* expansion methods. Although yields are similar to CB expansion methods, scalability of an iPSC source offers clear advantages over CB because of the capacity to manufacture large numbers of starting iPSC. Additionally, immunologically functional iPSC-derived DCs present distinct benefits over the standard practice of generating MoDCs from patient monocytes, including overcoming the dysfunction often seen in cancer patient monocytes or MoDCs,[9] enabling allogeneic off-the-shelf preparation that eliminates the need for patient-specific leukapheresis, and facilitating faster time-to-access with improved batch standardization and validation.

The terminally differentiated iPSC-derived DC by our method expressed the markers of all cDC subsets at the protein level; however, the mRNA expression profile of these cells showed a hybrid phenotype that was most similar to moDC. This inconsistency between gene and protein expression in our iPSC-DC subsets might be explained by differences in RNA and protein stability. Protein level depends not solely on mRNA levels, but also on translation rate and protein half-lives (reviewed by Buccitelli and Selbach[45]). High translational demand may result in low transcript even when the protein is detectable. Nonproliferative cells, such as our mature iPSC-DCs, have protein half-lives >500 h,[46] which may result in a stable protein level even when the gene is no longer actively transcribed.

The transcriptional analyses of iPSC-derived DC subsets highlight hybrid phenotype most similar to moDC, when compared with primary DCs in the Stemformatics DC and myeloid atlases. For example, iPSC-DC1 expressed genes classically associated with cDC1 subsets (eg *CLEC9A* and *CADM1*) but they also expressed DC2-markers (eg *CD1C*), so lacking the full identity of either subset. This hybrid identity has been previously seen in the culture of CB progenitors under FLT3L-driven differentiation,[18] and culture of primary progenitors has induced expression of the cDC2 marker, CD1C, in cDC1 subsets[47] and others have shown that iPSC-derived DC1 co-express XCR1 and CD14 markers.[40,48] This mixed phenotype might be attributed to the culture conditions which confuse the normal environmental signals, such that cultured cells may not engage the specific transcriptional network necessary for deriving a particular DC subset. To our knowledge, the generation of cDC1 from iPSC under a feeder-free culture system has not yet been achieved. Previous studies

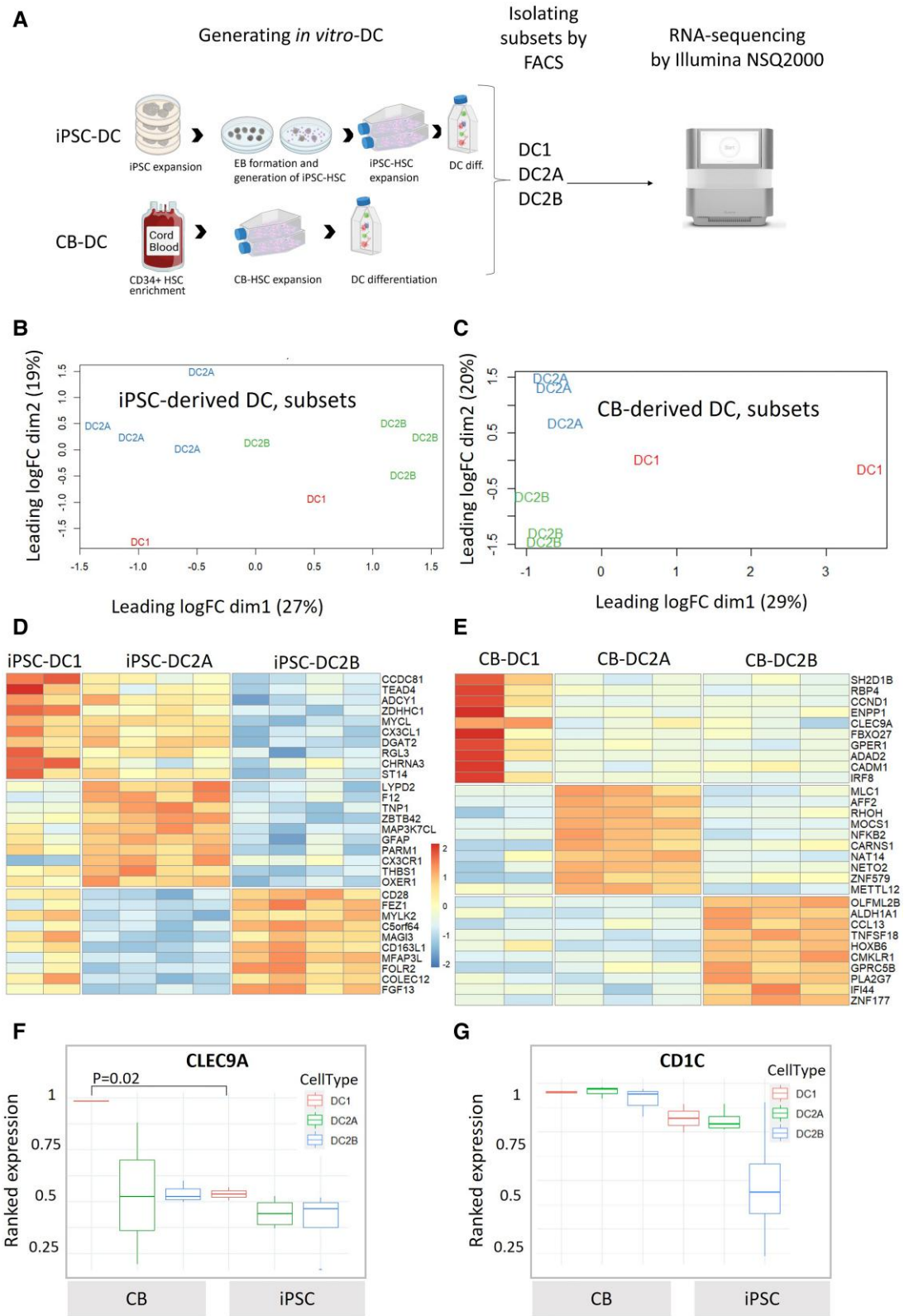

Fig. 5. Characterization of iPSC- and CB-derived DCs by bulk RNA-sequencing. a) Experimental setup of generation DCs from iPSC and CB. The process includes iPSC expansion, harvesting of hematopoietic stem cells (iPSC-HSC), expansion of iPSC-HSC, and differentiating to DCs. Similarly, CB-HSC were expanded and differentiated to DCs. Samples were FACS sorted and analysed by bulk RNAseq. b) MDS plot of log2 fold changes showing sample clustering of iPSC-derived dendritic cells (iPSC-DC). c) MDS plot of log2 fold changes showing sample clustering of cord blood CD34+-derived DC (CB-DC). d) Heatmap of DE genes by iPSC-DC subsets. The top 10 DE genes with p_adjust (BH) < 0.01 ranked with logFC were selected for heatmap display (See extended list in Table S9). e) Heatmap of DE genes by CB-DC subsets. The top 10 DE genes with p_adjust (BH) < 0.01 ranked with logFC were selected for heatmap display (See extended list in Table S10). f) CLEC9A ranked gene expression among iPSC-DC and CB-DC subsets. g) CD1C ranked gene expression among iPSC-DC and CB-DC subsets. *P*-value by unpaired 2-tailed student *T*-test.

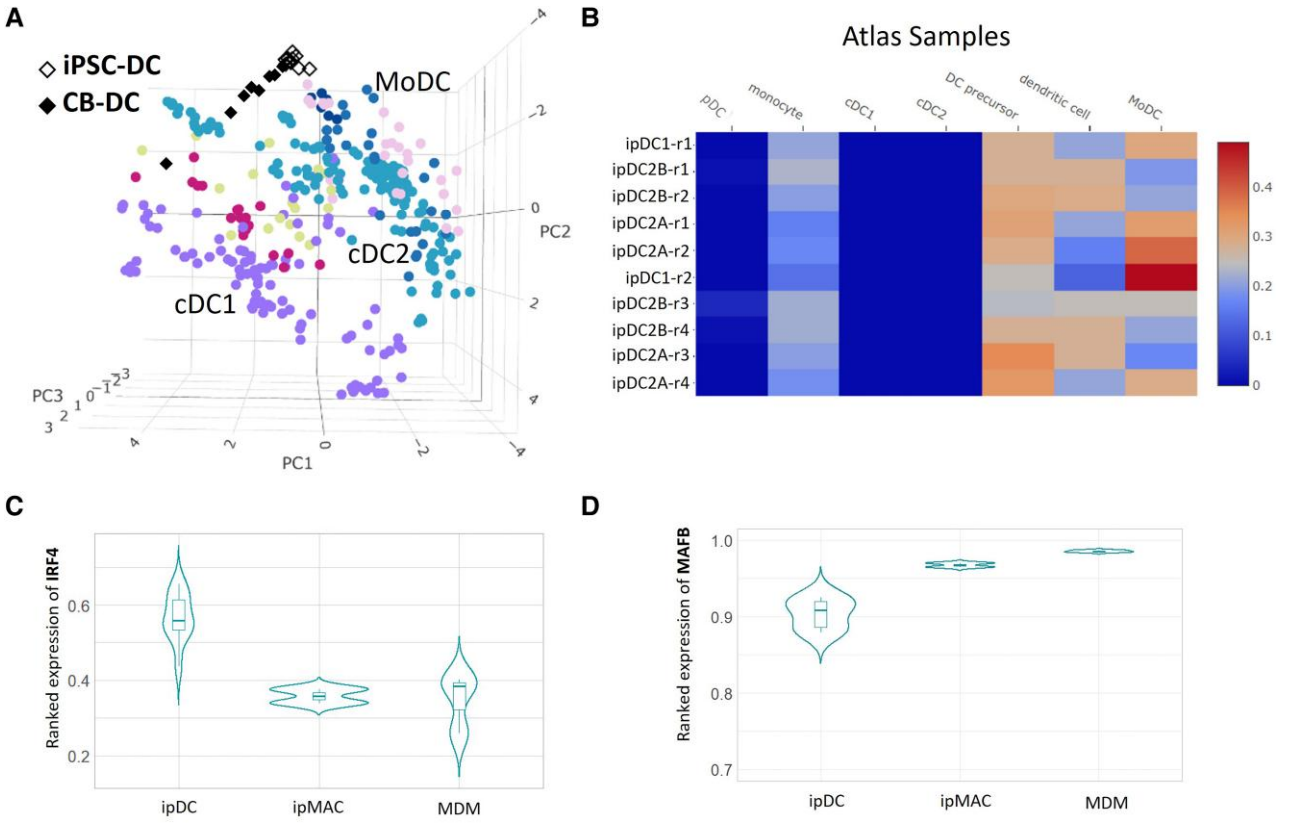

Fig. 6. Benchmarking iPSC-derived DCs against other myeloid cells. a) Projection of iPSC-DC on Human DC Atlas showing the proximity of iPSC-DC transcription with atlas MoDC subset. b) Capybara similarity scores between iPSC-DC and atlas cell types showing that iPSC-DC capture the MoDC transcriptional profile. c) Violin plot of ranked gene expression of IRF4, and d) MAFB transcription factors compared between our iPSC-derived DCs (ipDC) with external transcriptional data[29] on iPSC-derived macrophages (ipMAC) and MDM, previously obtained in our laboratory.

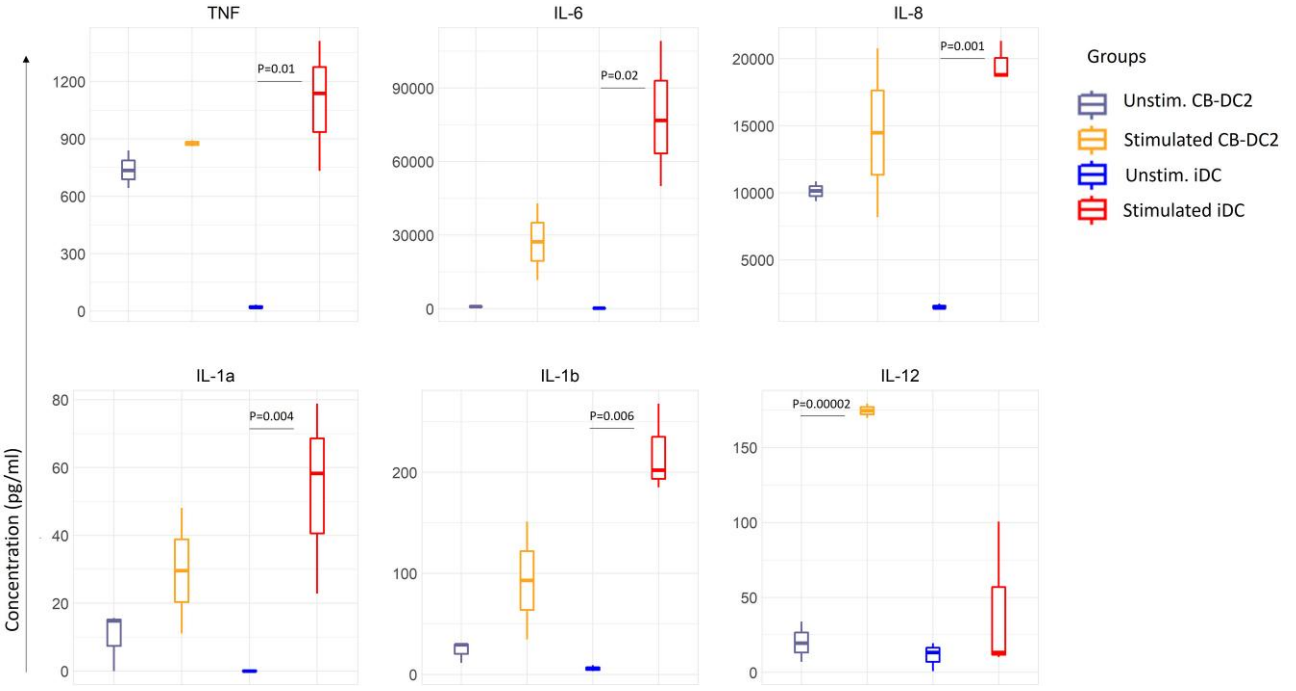

Fig. 7. iPSC-DCs stimulated by TLR adjuvants produce proinflammatory cytokines. FACS-sorted CD1c+ iPSC-DC and CD1c+ CD14– CB-DC2A were stimulated overnight (16 h) and assessed for secreted immune modulators by CBA. Three samples of iPSC-DCs are differentiated from HDF51 and PB001.1 lines. Three samples of CB-DC differentiated from CD34+ cord blood cells of 2 donors. *P*-values by paired 2-way student *T*-test.

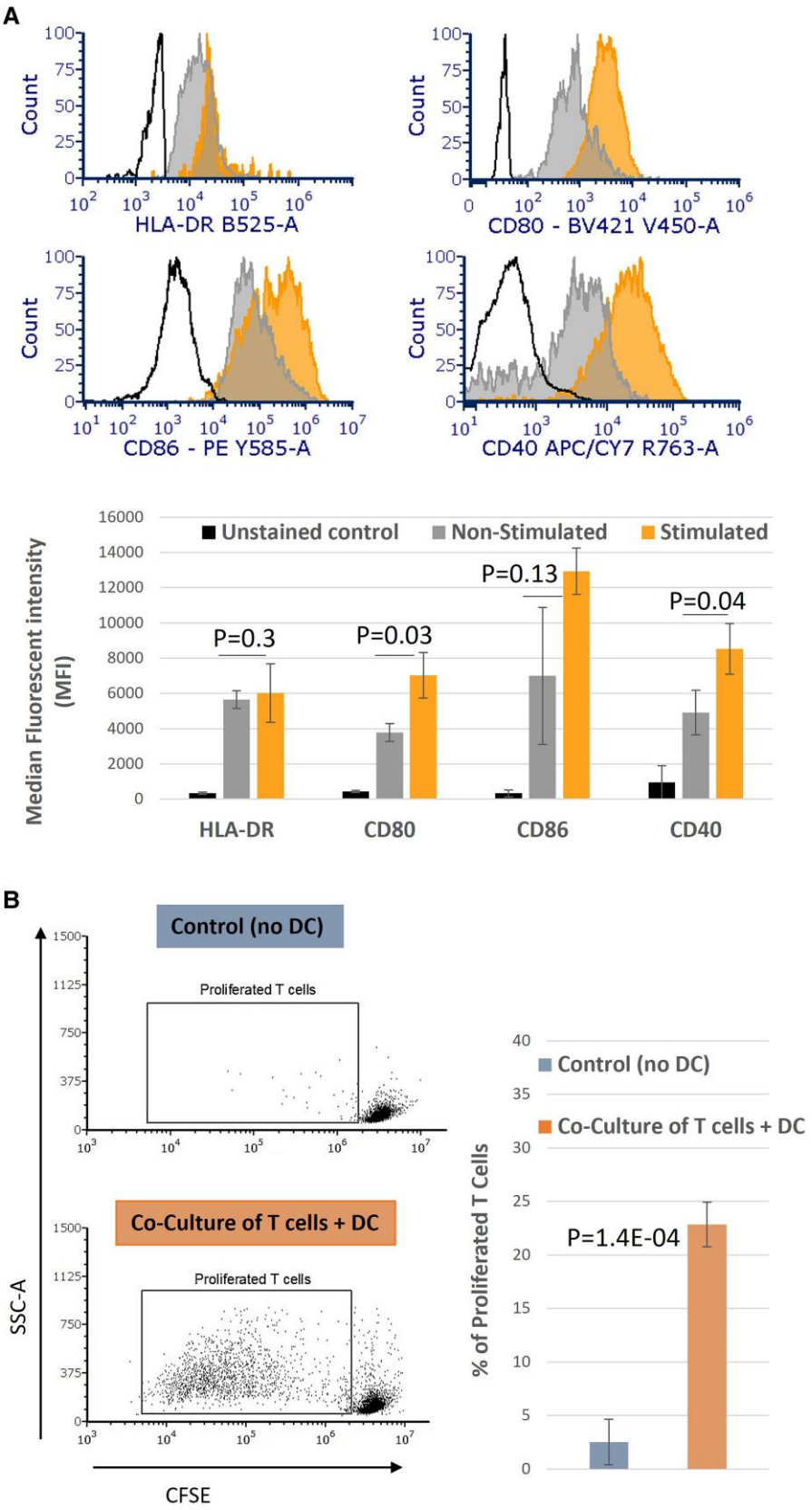

Fig. 8. iPSC-derived DCs respond to TLR and activate T cells. a) Analysis of MFI of HLA-DR and co-stimulatory molecules CD80, CD86, and CD40 between stimulated (by LPS and Poly:IC), unstimulated and unstained control samples of FACS sorted CD1c+ iPSC-DC in orange, gray, and black color, respectively. b) MLR analysis to assess the proliferation of pan-CD4/CD8 T cells in co-cultured samples (T cell+ DC) compared with control samples (only T cell, no DC). T cells are labeled with CellTracker CFSE to track their division. The number of replicates in each condition: $n = 3$. P-value by paired 2-way student T-test.

reported a MoDC/DC2-like profile from iPSC-DC[27,49,50] as well as the expression of monocytic marker *CD14* by their iPSC-derived DCs.[40,48]

Ultimately for clinical applications, and regardless of the source materials, reliable, scalable generation of progenitors is needed. This is particularly important for human DCs, which do not proliferate once mature. It is important that the in vitro-generated DC are functional—in that they are migratory to lymph nodes, can recognize pathogens, and are capable of processing and presentation of antigens to T-cells, while producing inflammatory cytokines that provide an instructive environment. Our stimulated in vitro iPSC-derived DCs appear to be able to produce proinflammatory cytokines, upregulate co-stimulatory and migration-associated molecules, and activate T cells. Further modifications to the protocol will be necessary ahead of clinical application—none of the reagents used here are cGMP certified, including the iPSC line itself. We used fetal bovine serum in the final stages of DC differentiation, so serum alternatives need to be evaluated in this system. Functional assessment of the iPSC-derived DC in vivo, including their longevity, capacity to migrate, and engagement with T cells in lymph nodes or peripheral tissues, has not yet been evaluated.

Acknowledgments

The authors thank the Melbourne Cytometry Platform at the University of Melbourne for infrastructure support, and the Hudson Genomics Facility, Hudson Institute of Medical Research, for assistance with RNA library preparation and sequencing.

Author contributions

Z.E. conceptualization, methodology, and writing the original draft. C.A.W. Supervision, conceptualization, writing—review and editing. V.J. Formal analysis, writing—review and editing. M.S. Formal analysis, writing—review and editing. S.K.B. Data curation, writing—review and editing. K.J.R. Supervision, methodology. J.D.M. Supervision, writing—review and editing.

Supplementary material

Supplementary material is available at *Journal of Leukocyte Biology* online.

Funding

This work was supported by the National Health and Medical Research Council Australia APP1186371 to C.A.W. The authors thank the Melbourne Cytometry Platform at the University of Melbourne for infrastructure support, and the Hudson Genomics Facility, Hudson Institute of Medical Research, for assistance with RNA library preparation and sequencing.

Conflicts of interest. None declared.

References

1. Kvedaraite E, Ginhoux F. Human dendritic cells in cancer. *Sci Immunol*. 2023:7:eabm9409. https://doi.org/10.1126/sciimmunol.abm9409
2. Schreibelt G, *et al.* Effective clinical responses in metastatic melanoma patients after vaccination with primary myeloid dendritic cells. *Clin cancer Res*. 2016;22:2155–2166. https://doi.org/10.1158/1078-0432.CCR-15-2205
3. Dey M, *et al.* Dendritic cell–based vaccines that utilize myeloid rather than plasmacytoid cells offer a superior survival advantage in malignant glioma. *J Immunol*. 2015:195:367–376. https://doi.org/10.4049/jimmunol.1401607
4. Wculek SK, *et al.* Dendritic cells in cancer immunology and immunotherapy. *Nat Rev Immunol*. 2020:20:7–24. https://doi.org/10.1038/s41577-019-0210-z
5. Bachem A, *et al.* Superior antigen cross-presentation and XCR1 expression define human CD11c+ CD141+ cells as homologues of mouse CD8+ dendritic cells. *J Exp Med*. 2010:207:1273–1281. https://doi.org/10.1084/jem.20100348
6. Jongbloed SL, *et al.* Human CD141+ (BDCA-3)+ dendritic cells (DCs) represent a unique myeloid DC subset that cross-presents necrotic cell antigens. *J Exp Med*. 2010:207:1247–1260. https://doi.org/10.1084/jem.20092140
7. Laoui D, *et al.* The tumour microenvironment harbours ontogenically distinct dendritic cell populations with opposing effects on tumour immunity. *Nat Commun*. 2016:7:13720. https://doi.org/10.1038/ncomms13720
8. Salmon H, *et al.* Expansion and activation of CD103+ dendritic cell progenitors at the tumor site enhances tumor responses to therapeutic PD-L1 and BRAF inhibition. *Immunity*. 2016:44:924–938. https://doi.org/10.1016/j.immuni.2016.03.012
9. Johnson P, Rosendahl N, Radford KJ. Conventional type 1 dendritic cells (cDC1) as cancer therapeutics: challenges and opportunities. *Expert Opin Biol Ther*. 2022:22:465–472. https://doi.org/10.1080/14712598.2022.1994943
10. Bedke N, *et al.* A method for the generation of large numbers of dendritic cells from CD34+ hematopoietic stem cells from cord blood. *J Immunol Methods*. 2020:477:112703. https://doi.org/10.1016/j.jim.2019.112703
11. Collin M, Bigley V. Human dendritic cell subsets: an update. *Immunology*. 2018:154:3–20. https://doi.org/10.1111/imm.12888
12. Sallusto F, Lanzavecchia A. Efficient presentation of soluble antigen by cultured human dendritic cells is maintained by granulocyte/macrophage colony-stimulating factor plus interleukin 4 and downregulated by tumor necrosis factor alpha. *J Exp Med*. 1994:179:1109–1118. https://doi.org/10.1084/jem.179.4.1109
13. Le Naour F, *et al.* Profiling changes in gene expression during differentiation and maturation of monocyte-derived dendritic cells using both oligonucleotide microarrays and proteomics. *J Biol Chem*. 2001:276:17920–17931. https://doi.org/10.1074/jbc.M100156200
14. Tanaka H, Demeure CE, Rubio M, Delespesse G, Sarfati M. Human monocyte–derived dendritic cells induce naive T cell differentiation into T helper cell type 2 (Th2) or Th1/Th2 effectors: role of stimulator/responder ratio. *J Exp Med*. 2000:192:405–412. https://doi.org/10.1084/jem.192.3.405
15. Heras-Murillo I, Adán-Barrientos I, Galán M, Wculek SK, Sancho D. Dendritic cells as orchestrators of anticancer immunity and immunotherapy. *Nat Rev Clin Oncol*. 2024:21:257–277. https://doi.org/10.1038/s41571-023-00821-7
16. Sugimoto C, *et al.* Differentiation kinetics of blood monocytes and dendritic cells in macaques: insights to understanding human myeloid cell development. *J Immunol*. 2015:195:1774–1781. https://doi.org/10.4049/jimmunol.1500522
17. Patel AA, *et al.* The fate and lifespan of human monocyte subsets in steady state and systemic inflammation. *J Exp Med*. 2017:214:1913–1923. https://doi.org/10.1084/jem.20170355
18. Balan S, *et al.* Human XCR1+ dendritic cells derived in vitro from CD34+ progenitors closely resemble blood dendritic cells, including their adjuvant responsiveness, contrary to monocyte-derived dendritic cells. *J Immunol*. 2014:193:1622–1635. https://doi.org/10.4049/jimmunol.1401243

19. Poulin LF, *et al.* Characterization of human DNGR-1+ BDCA3+ leukocytes as putative equivalents of mouse CD8α+ dendritic cells. *J Exp Med*. 2010:207:1261–1271. https://doi.org/10.1084/jem.20092618
20. Thordardottir S, *et al.* Hematopoietic stem cell-derived myeloid and plasmacytoid DC-based vaccines are highly potent inducers of tumor-reactive T cell and NK cell responses ex vivo. *Oncoimmunology*. 2017:6:e1285991. https://doi.org/10.1080/2162402X.2017.1285991
21. Thordardottir S, *et al.* The aryl hydrocarbon receptor antagonist StemRegenin 1 promotes human plasmacytoid and myeloid dendritic cell development from CD34+ hematopoietic progenitor cells. *Stem Cells Dev*. 2014:23:955–967. https://doi.org/10.1089/scd.2013.0521
22. Anselmi G, *et al.* Engineered niches support the development of human dendritic cells in humanized mice. *Nat Commun*. 2020:11:2054. https://doi.org/10.1038/s41467-020-15937-y
23. van Eck van der Sluijs J, *et al.* Clinically applicable CD34+-derived blood dendritic cell subsets exhibit key subset-specific features and potently boost anti-tumor T and NK cell responses. *Cancer Immunol Immunother*. 2021:70:3167–3181. https://doi.org/10.1007/s00262-021-02899-3
24. Maier B, *et al.* A conserved dendritic-cell regulatory program limits antitumour immunity. *Nature*. 2020:580:257–262. https://doi.org/10.1038/s41586-020-2134-y
25. Satoh T, *et al.* Human DC3 antigen presenting dendritic cells from induced pluripotent stem cells. *Front Cell Dev Biol*. 2021:9:667304. https://doi.org/10.3389/fcell.2021.667304
26. Monkley S, *et al.* Optimised generation of iPSC-derived macrophages and dendritic cells that are functionally and transcriptionally similar to their primary counterparts. *PLoS One*. 2020:15:e0243807. https://doi.org/10.1371/journal.pone.0243807
27. Alsinet C, *et al.* Robust temporal map of human in vitro myelopoiesis using single-cell genomics. *Nat Commun*. 2022:13:1–17. https://doi.org/10.1038/s41467-022-30557-4
28. Makino K, *et al.* Generation of cDC-like cells from human induced pluripotent stem cells via notch signaling. *J Immunother Cancer*. 2022:10:e003827. https://doi.org/10.1136/jitc-2021-003827
29. Rajab N, *et al.* An integrated analysis of human myeloid cells identifies gaps in in vitro models of in vivo biology. *Stem Cell Reports*. 2021:16:1629–1643. https://doi.org/10.1016/j.stemcr.2021.04.010
30. Vlahos K, *et al.* Generation of iPSC lines from peripheral blood mononuclear cells from 5 healthy adults. *Stem Cell Res*. 2019:34:101380. https://doi.org/10.1016/j.scr.2018.101380
31. Jones JC, *et al.* Melanocytes derived from transgene-free human induced pluripotent stem cells. *J Invest Dermatol*. 2013:133:2104. https://doi.org/10.1038/jid.2013.139
32. Ng ES, Davis R, Stanley EG, Elefanty AG. A protocol describing the use of a recombinant protein-based, animal product-free medium (APEL) for human embryonic stem cell differentiation as spin embryoid bodies. *Nat Protoc*. 2008:3:768–776. https://doi.org/10.1038/nprot.2008.42
33. Nafria M, Bonifer C, Stanley EG, Ng ES, Elefanty AG. Protocol for the generation of definitive hematopoietic progenitors from human pluripotent stem cells. *STAR Protoc*. 2020:1:100130. https://doi.org/10.1016/j.xpro.2020.100130
34. Marks ZRC, *et al.* Interferon-ϵ is a tumour suppressor and restricts ovarian cancer. *Nature*. 2023:620:1063–1070. https://doi.org/10.1038/s41586-023-06421-w
35. Choi J, *et al.* Stemformatics: visualize and download curated stem cell data. *Nucleic Acids Res*. 2019:47:D841–D846. https://doi.org/10.1093/nar/gky1064
36. Ritchie ME, *et al.* Limma powers differential expression analyses for RNA-sequencing and microarray studies. *Nucleic Acids Res*. 2015:43:e47–e47. https://doi.org/10.1093/nar/gkv007
37. McCarthy DJ, Chen Y, Smyth GK. Differential expression analysis of multifactor RNA-Seq experiments with respect to biological variation. *Nucleic Acids Res*. 2012:40:4288–4297. https://doi.org/10.1093/nar/gks042
38. Wickham H, Chang W, Wickham MH. Package 'ggplot2'. *Creat Elegant Data Vis Using Gramm Graph Version*. 2016:2:1–189. ISBN-13: 978-3319242750.
39. Bates D. Fitting linear mixed models in R. *R News*. 2005:5:27–30. https://journal.r-project.org/articles/RN-2005-005/#citation
40. Sachamitr P, Leishman AJ, Davies TJ, Fairchild PJ. Directed differentiation of human induced pluripotent stem cells into dendritic cells displaying tolerogenic properties and resembling the CD141+ subset. *Front Immunol*. 2018:8:1935. https://doi.org/10.3389/fimmu.2017.01935
41. Elahi Z, *et al.* The human dendritic cell atlas: an integrated transcriptional tool to study human dendritic cell biology. *J Immunol*. 2022:209:2352–2361. https://doi.org/10.4049/jimmunol.2200366
42. Goudot C, *et al.* Aryl hydrocarbon receptor controls monocyte differentiation into dendritic cells versus macrophages. *Immunity*. 2017:47:582–596. https://doi.org/10.1016/j.immuni.2017.08.016
43. Nizzoli G, *et al.* IL-10 promotes homeostatic proliferation of human CD8+ memory T cells and, when produced by CD1c+ DCs, shapes naive CD8+ T-cell priming. *Eur J Immunol*. 2016:46:1622–1632. https://doi.org/10.1002/eji.201546136
44. Leal Rojas IM, *et al.* Human blood CD1c+ dendritic cells promote Th1 and Th17 effector function in memory CD4+ T cells. *Front Immunol*. 2017:8:971. https://doi.org/10.3389/fimmu.2017.00971
45. Buccitelli C, Selbach M. mRNAs, proteins and the emerging principles of gene expression control. *Nat Rev Genet*. 2020:21:630–644. https://doi.org/10.1038/s41576-020-0258-4
46. Mathieson T, *et al.* Systematic analysis of protein turnover in primary cells. *Nat Commun*. 2018:9:689. https://doi.org/10.1038/s41467-018-03106-1
47. Kirkling ME, *et al.* Notch signaling facilitates in vitro generation of cross-presenting classical dendritic cells. *Cell Rep*. 2018:23:3658–-3672.e6. https://doi.org/10.1016/j.celrep.2018.05.068
48. Silk KM, *et al.* Cross-presentation of tumour antigens by human induced pluripotent stem cell-derived CD141 XCR1 dendritic cells. *Gene Ther*. 2012:19:1035–1040. https://doi.org/10.1038/gt.2011.177
49. Choi K-D, Vodyanik M, Slukvin II. Hematopoietic differentiation and production of mature myeloid cells from human pluripotent stem cells. *Nat Protoc*. 2011:6:296–313. https://doi.org/10.1038/nprot.2010.184
50. Senju S, *et al.* Generation of dendritic cells and macrophages from human induced pluripotent stem cells aiming at cell therapy. *Gene Ther*. 2011:18:874–883. https://doi.org/10.1038/gt.2011.22